Case Studies in Construction Materials 23 (2025) e05243

Contents lists available at ScienceDirect

Case Studies in Construction Materials

journal homepage: www.elsevier.com/locate/cscm

Automated ensemble learning for shear strength prediction in marine reinforced concrete slabs: A self-optimizing stacked framework

Jingyu Wei [a], Bingcheng Chen [a], Bin Jia [a], Zi-yue Gao [b], Peng Xia [a], Kai-Di Peng [c], Junwei Ren [d,*], Xiao-Hua Ji [a], Zi-jian Sui [e]

[a] College of Civil Engineering and Architecture, Zhejiang University, Hangzhou 310058, China
[b] The Key Laboratory of Road and Traffic Engineering, Ministry of Education, Tongji University, Shanghai 200092, China
[c] Department of Civil and Environmental Engineering, The Hong Kong Polytechnic University, 999077, Hong Kong, China
[d] College of Urban Construction, Zhejiang Shuren University, Hangzhou 310015, China
[e] Liaoning Gongtou Construction Co., Ltd., Tieling 112008, China

ARTICLE INFO

Keywords:
Punching shear strength
Reinforced concrete slabs
Automated machine learning
Structural failure prediction
Marine structures

ABSTRACT

Reinforced concrete (RC) slabs are fundamental structural elements widely employed in both general and marine engineering applications, where they are required to ensure load distribution and in-plane stability under various environmental and mechanical stresses. In marine environments, these slabs are particularly vulnerable to degradation mechanisms such as chloride-induced corrosion and cyclic wave loading, which significantly increase the risk of brittle punching shear failures. Such failures, typically resulting from unbalanced shear forces and insufficient reinforcement detailing, can lead to abrupt and catastrophic structural collapse. Existing empirical approaches for predicting punching shear strength often lack the capacity to account for the complex, nonlinear interactions among geometric, material, and environmental parameters, thereby limiting their reliability in marine contexts. To address these limitations, this study proposes an automated machine learning (AutoML) framework that leverages data-driven modeling for accurate and efficient prediction of punching shear strength in RC slabs. The framework integrates automated model selection, hyperparameter optimization, and feature selection within a self-optimizing multi-layer stacking ensemble, eliminating the need for manual intervention and enhancing predictive performance. Model interpretability is achieved through SHapley Additive exPlanations (SHAP) analysis, which identifies the most influential predictors and provides insights into underlying structural behaviors. The proposed methodology is validated using an extensive dataset comprising RC slabs with varying reinforcement configurations, material properties, and exposure conditions, including those specific to marine environments. Results demonstrate superior generalization capability and improved prediction accuracy compared to traditional approaches, highlighting the framework's potential as a practical tool for structural design, assessment, and durability analysis of RC elements in marine infrastructure systems.

* Corresponding author.
E-mail address: junweiren@zjsru.edu.cn (J. Ren).

https://doi.org/10.1016/j.cscm.2025.e05243
Received 2 July 2025; Received in revised form 15 August 2025; Accepted 28 August 2025
Available online 30 August 2025

1. Introduction

Reinforced Concrete (RC) slabs play a crucial role as structural components in construction and civil engineering, characterized by the synergistic interaction between concrete and steel reinforcement to form flat elements [1–5]. These slabs are primarily designed to support and distribute loads, providing essential horizontal stability and load-bearing capabilities. In marine structures—such as offshore platforms, coastal bridges, and quay decks—RC slabs are particularly critical due to their exposure to harsh environments involving salt spray, wave impact, and long-term chloride-induced corrosion. These conditions significantly accelerate deterioration mechanisms, thereby increasing the vulnerability of RC slabs to punching shear failures.

RC flat slabs are vulnerable to brittle punching and shearing failures when exposed to unbalanced shear forces and bending moments between the slab and its supporting columns [6]. Such failures often arise from inadequate shear resistance or the lack of transverse reinforcing bars, which can lead to localized stress concentrations. In the event of brittle shear failure, shear cracks develop on the surface of the slab, following the direction of the shear force. This results in a sudden and rapid failure, characterized by minimal plastic deformation [7]. The localized nature of this failure not only reduces the load-bearing capacity but may also trigger progressive collapse, compromising the overall structural integrity. This risk is particularly heightened in marine structures, where combined mechanical and chemical stressors can reduce residual strength far below design expectations. Therefore, accurate prediction of punching shear strength is essential to ensure the safety and long-term durability of RC slabs in both conventional and marine environments.

Through a significant number of studies, the punching shear resistance of reinforced concrete (RC) flat slabs has been researched since the 1950s [8,9]. Einpaul et al. [10] created an empirical formula for punching shear strength, which is frequently used in ACI's specifications, after conducting a significant number of experiments and having several researchers analyze the data. Additionally, they carried out field experiments on RC slabs with various shear reinforcement, various shapes, and various parameters, as well as slabs with various materials and various types of reinforcement, to look into the variation of punching shear strength [11–15]. By using numerical simulation and the theory of critical shear fractures as a foundation, they proposed a new criterion of punching-shear damage for the research of shear cracks, and the performance of reinforced concrete flat slabs was improved by various reinforcement techniques [16–19]. While these traditional approaches have advanced design practice, they often rely on empirical assumptions that may not fully capture the nonlinear interactions between influencing variables. This limitation is even more pronounced under the complex exposure conditions encountered in marine environments. As structural systems and loading conditions become more complex, there is a growing demand for advanced predictive tools that can accommodate multivariate dependencies.

Recently, machine learning algorithms have gained traction in structural engineering research for predicting shear strength and quantifying damage in concrete structures. One of the pioneering artificial neural network (ANN) models for estimating the punching shear capacity of RC slabs was developed by Elshafey et al. [20] and Said et al. [21]. Concurrently, Gandomi and Roke [22] focused on identifying variables related to punching shear that could lead to overfitting in ANN models. Tran and Kim [23] made significant contributions by proposing new ANN-based equations for forecasting punching shear resistance. Additionally, Chetchotisak et al. [24] introduced an innovative punching shear strength equation and its corresponding strength resistance factor, tailored specifically for practical design applications, utilizing the RA1 approach. The recent popularity of machine learning methods for predicting punching shear strength is further exemplified by Nguyen et al. [25], who explored the gradient boosting technique XGBoost, demonstrating its superior performance compared to traditional ANN and random forest (RF) models. Supporting this, Mangalathu et al. [26] compared the performance of seven machine learning techniques, including support vector machine (SVM), decision tree (DT), RF, AdaBoost, XGBoost, k-nearest neighbors (kNN), and RA5, highlighting the effectiveness of advanced algorithms. Furthermore, machine learning techniques have been adapted to estimate the punching shear strengths of various concrete slab types, including RC slabs reinforced with steel fibers [27–29] and those incorporating fiber-reinforced polymer (FRP) bars [30]. Faridmehr et al. [31] developed a unique information bat neural network model to forecast the punching shear capacity of RC flat slabs without shear reinforcement.

Despite advancements in machine learning (ML)-based shear strength prediction models, their implementation often requires manual modeling processes, compromising efficiency and accuracy in engineering applications. Typically, multiple ML models are deployed on a given dataset, with the one yielding the highest accuracy selected as optimal. This process must be repeated for different structural elements or materials, and a single model may not consistently deliver satisfactory accuracy across diverse shear strength prediction scenarios. Such manual modeling not only proves inefficient but can also introduce model bias [5,32–36], diminishing the reliability of ML-based predictions. In contrast, automated machine learning (AutoML) streamlines the entire modeling process, encompassing data preprocessing, feature selection, model selection, and hyperparameter tuning [37–39]. AutoML systems efficiently explore a broad array of algorithms and hyperparameters, optimizing model performance with minimal human intervention, which accelerates model development while enhancing prediction accuracy and generalization capability. These benefits are also can be advantageous for marine infrastructure, where real-time decision-making, limited data quality, and the need for robust prediction under uncertainty are prevalent challenges. This study proposes an AutoML-based framework for predicting the punching shear strength of RC slabs, utilizing a multi-layer stacking ensemble to integrate multiple base learners. Unlike traditional single-model approaches, this method eliminates manual intervention and enhances prediction performance by leveraging model diversity. Its design is intended to be applicable across a variety of structural conditions, including those influenced by marine exposure, thus contributing to safer and more resilient coastal and offshore infrastructure systems.

This study aims to conduct a comprehensive analysis of reinforced concrete (RC) slab shear strength prediction using automated machine learning (AutoML) techniques. Section 2 provides an overview of the database sources, outlining the data collection methods and the characteristics of the dataset utilized in this research. In Section 3, we offer a detailed description of the various machine learning methodologies employed, including both base machine learning models and AutoML approaches, along with the criteria used

to select the optimal method for the prediction task. Section 4 focuses on the performance evaluation of the machine learning models, featuring an extensive error analysis and a thorough assessment of their predictive accuracy. Section 5 presents the AutoML-based SHAP (SHapley Additive exPlanations) analysis, which includes an in-depth examination of feature importance and sensitivity analysis to gain insights into the factors influencing shear strength predictions. Finally, Section 6 describes the development of a graphical user interface (GUI) that enables shear strength predictions from user-specified input parameters, highlighting the model's usability in both research and practice.

2. Database description

2.1. Database

The dataset underpinning this investigation is sourced from an established repository housing 380 two-way RC slabs lacking transverse reinforcement at internal supports, accessible at https://datacenterhub.org/resources/256. Within this comprehensive database, 519 meticulously documented test samples encompass detailed information pertaining to test configurations, sample geometries, material properties, and test outcomes. The principal aim of this study is to develop a bespoke machine learning model designed to accurately estimate the maximum shear strength of plate elements when subjected to punching shear damage in the absence of transverse reinforcement. Specifically, from the extensive dataset, a subset comprising 380 samples was thoughtfully selected to delve into the nuanced shear strength characteristics of these plate elements. In this research study, eight distinct design factors were meticulously selected as the primary variables for examination. Table 1 shows the characteristics of the input variables. These parameters encompass the equivalent column width (b), slab height (h), effective depth (d), critical perimeter (bo), shear span (a), density (rho), yield strength of flexural reinforcement (fy), and compressive strength (fc).

2.2. Input and output variables

Fig. 1 shows distribution and correlation of input and output variables. These specified inputs are integral in determining the study's output, namely the shear strength.

3. Machine learning-based punching shear strength models

The fundamentals of seven prevalent machine learning algorithms are elaborated upon (Fig. 2).

3.1. Machine learning (ML)

This study employs seven machine learning models - Neural Network (NN), K-Nearest Neighbors (KNN), Extra Trees (XT), XGBoost, LightGBM, Random Forest (RF), and AutoML - selected for their complementary strengths in predicting shear strength of marine concrete structures. The ensemble methods (XT, XGBoost, LightGBM, RF) excel at capturing complex nonlinear relationships while mitigating overfitting, crucial for handling noisy marine environment data. KNN provides local pattern verification, NN models high-dimensional nonlinear mappings, and AutoML optimizes hyperparameters objectively. This diversified approach, validated in structural engineering applications, ensures robust prediction across varying marine conditions.

The NN model is a powerful approach capable of capturing intricate patterns in high-dimensional data through a layered architecture that iteratively adjusts weights via gradient descent, allowing it to generalize well across a range of input features [40]. KNN complements this by classifying or predicting target values based on proximity to known data points, making it particularly effective in scenarios where local data density plays a crucial role [41–43].

XT and RF both excel in ensemble learning, utilizing multiple decision trees to boost model performance by reducing overfitting and enhancing stability. XT differs from RF in its randomization during both feature selection and splitting criteria, leading to a more diverse set of trees [44], while RF aggregates predictions from a large number of decision trees to enhance robustness and predictive consistency [45].

XGBoost and LightGBM represent advanced gradient-boosting techniques that efficiently handle non-linear relationships in data through an ensemble of weak learners. XGBoost is known for its regularization capabilities, which prevent overfitting and enhance

Table 1
The data distribution of each variable in the database (kN).

Inputs	mean	std	max	min	mode	median
b	181.42	92.39	707.64	40.06	200.00	173.57
h	137.83	67.72	550.00	0.00	152.00	130.00
d	112.91	58.30	500.00	30.00	114.00	107.00
bo	1177.30	515.36	3904.00	312.62	562.00	1116.00
a	648.16	318.60	2320.00	38.00	270.00	675.00
rho	0.01	0.01	0.04	0.00	0.01	0.01
fy	469.79	118.28	749.00	250.00	550.00	471.00
fc	368.41	18.51	118.70	8.66	24.89	28.00

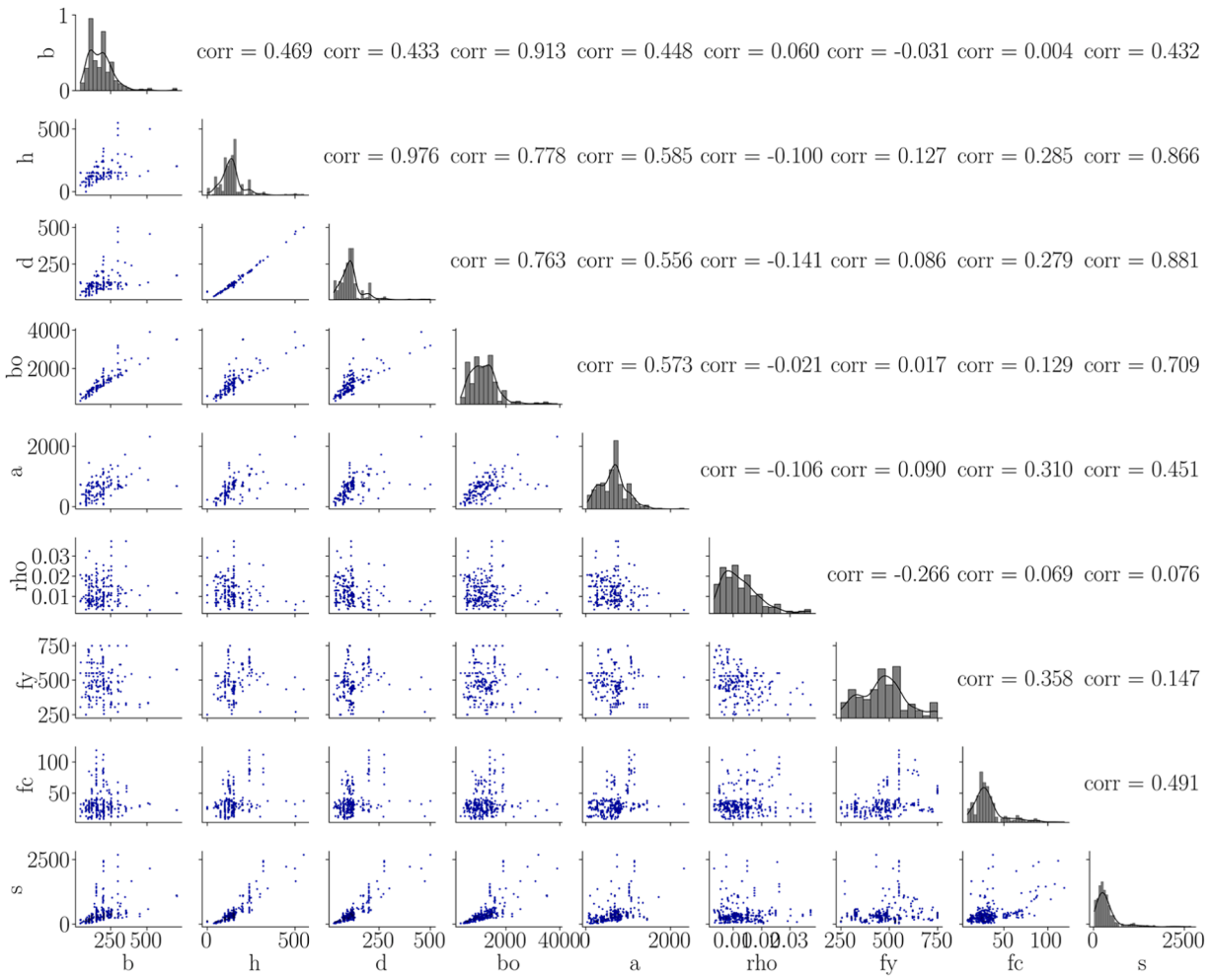

Fig. 1. Input and output variables distribution and correlation.

model accuracy [46,47], while LightGBM is optimized for high-speed training and low memory consumption, making it especially well-suited for large-scale datasets and real-time prediction scenarios [45]. Both models excel in addressing the challenges posed by the high-dimensional and multi-variable datasets commonly encountered in wind prediction studies.

3.2. Automatic machine learning (AutoML)

AutoML streamlines machine learning development by automating tasks such as data preprocessing, feature engineering, model selection, hyperparameter tuning, and ensembling, making machine learning accessible to non-experts. Techniques like Bayesian optimization, genetic algorithms, and neural architecture search help identify optimal model configurations, minimizing human intervention and accelerating deployment [45].

This study utilizes a multi-layer stacking framework, where predictions from lower-layer models feed into higher layers, combining base models' strengths and original features to enhance performance. k-fold bagging further reduces overfitting, and hyperparameters are automatically tuned via Bayesian optimization, allowing for rapid implementation without specialized ML knowledge.

3.3. Evaluation metrics

In the pursuit of optimizing the machine learning model, the dataset undergoes partitioning into distinct subsets: a training set and a test set. The training set, encompassing 70 % of the data, is harnessed for constructing the predictive model, while the model's performance evaluation unfolds on the remaining 30 % of the data. This evaluation scrutinizes the model's ability to forecast unseen instances, concurrently monitoring for indications of overfitting. Central to this assessment are pivotal metrics such as root mean square error (RMSE), variance (R^2), and mean absolute error (MAE), computed on the randomly allocated training set. These metrics furnish essential insights into the model's accuracy, resilience, and generalization prowess [48–50]. The calculation formulas for these

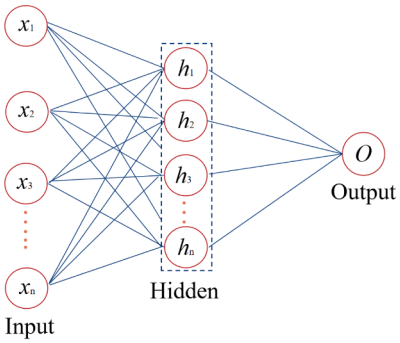

(a) Neural network (NN)

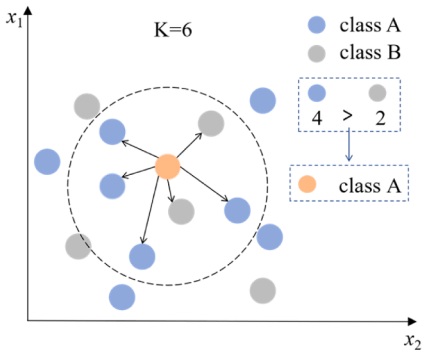

(b) K-Nearest Neighbor (KNN)

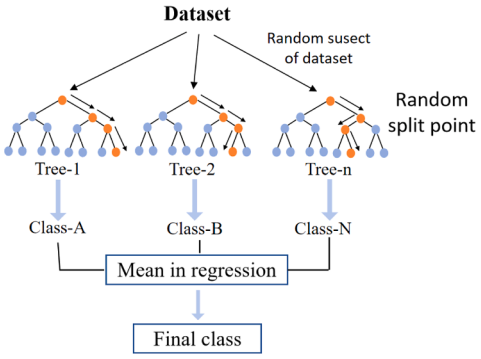

(c) Extra Trees (XT)

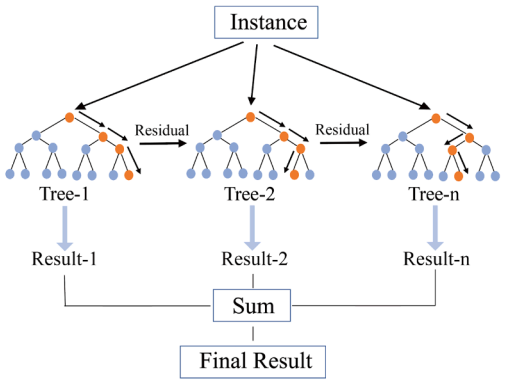

(d) Extreme gradient boosting (XGB)

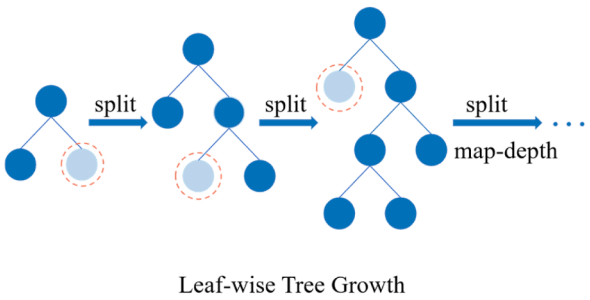

(e) Light GBM

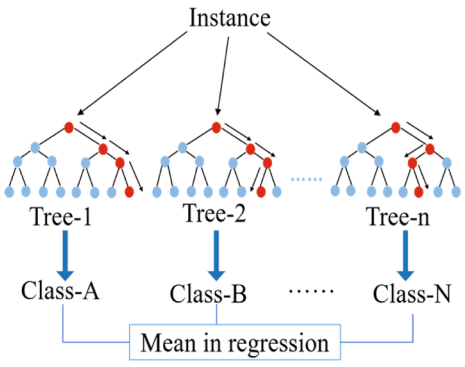

(f) Random forest (RF)

Fig. 2. The fundamental principles of ML models.

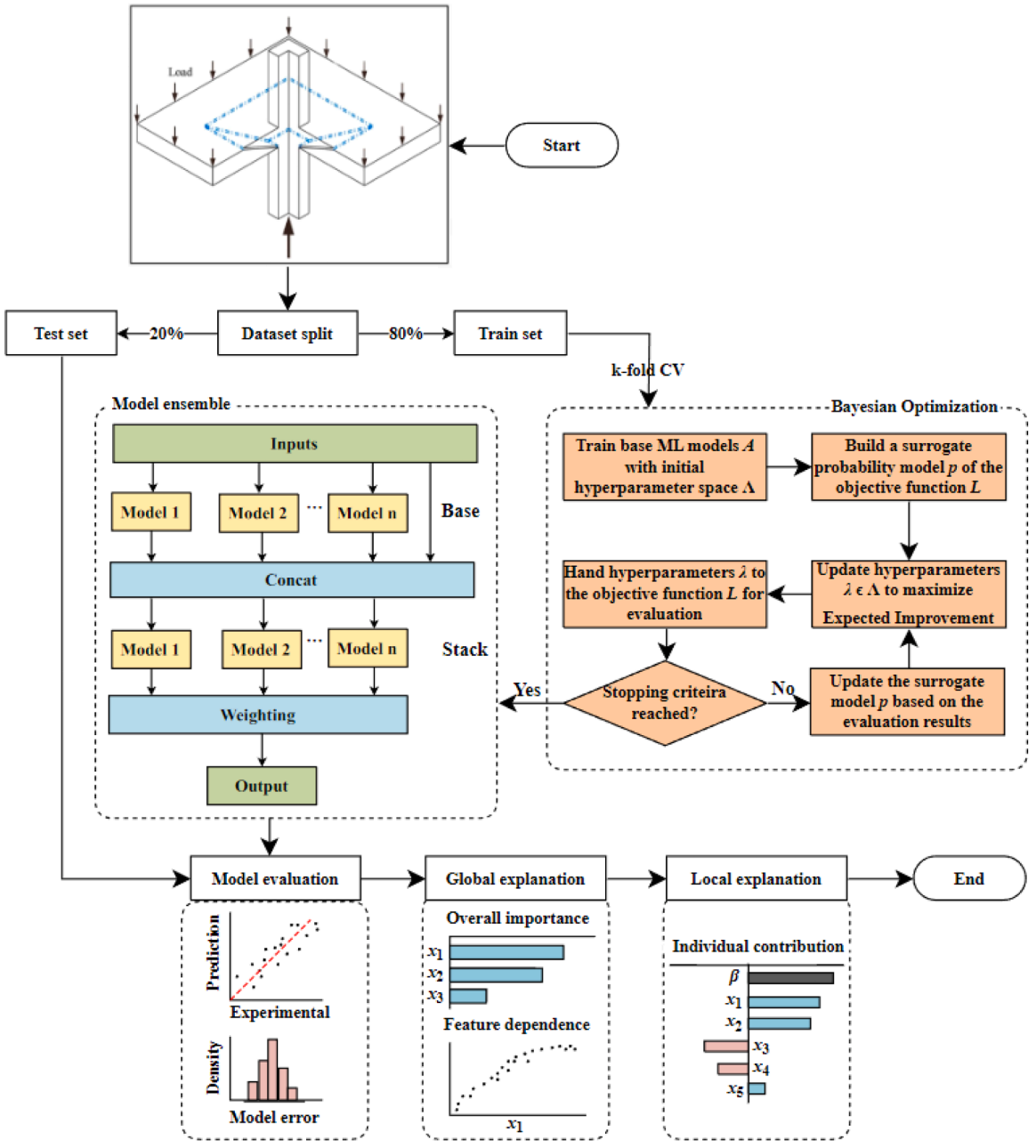

(g) Auto Machine learning (AutoML)

Fig. 2. (*continued*).

metrics are outlined below:

$$R^2 = \frac{\sum_{i=1}^{n}(x_i - \overline{x_i})(y_i - \overline{y_i})}{\sqrt{\sum_{i=1}^{n}(x_i - \overline{x_i})^2}\sqrt{\sum_{i=1}^{n}(y - \overline{y_i})^2}} \quad (3)$$

$$RMSE = \sqrt{\frac{\sum_{i=1}^{n}(x_i - y_i)^2}{n}} \tag{4}$$

$$MAE = \frac{\sum_{i=1}^{n}|x_i - y_i|}{n} \tag{5}$$

where x_i and y_i stand for the i_{th} output's expected and experimental values, respectively; $\overline{x_i}$and $\overline{y_i}$ also stand for the mean of the predicted and experimental values, respectively; and n stands for the quantity of data points. The R^2 number should be close to 1 for best accuracy. An R^2 of more than 0.8 has previously been shown to be acceptable, and studies have shown that this is associated with decreased MAE and RMSE values and higher prediction accuracy for the chosen model [51,52].

4. Performance of ML models

4.1. The deployment process of AutoML

The deployments process of an ML model mainly consists of model selection and hyperparameter optimization. Both steps are performed automatically without manual intervention for the proposed model. The number of layers for the multi-layer stacking framework is determined based on the complexity of the dataset. The single hyperparameter that needs to be discussed in this section for AutoML is training time. With more provided training time, the AutoML model will repeat the bagging process. The default training time enables all base models to finish training without repeating bagging. The values of 5-fold cross-validation against training time are illustrated in Fig. 3. R^2 of the train set reaches the peak value of 0.995 at 50 s, while the validation set yields the peak value of 0.957 at 300 s. The default training time for one circle is 150 s, indicating that stacking impacts more largely the model performance than bagging. Considering the balance between accuracy and efficiency, 150 s is an appropriate training time. In all trials, AutoML maintains the best model performance compared with other models, which demonstrates the usefulness of the adopted stacking framework in AutoML to avoid manually choosing a single model and improving model accuracy at the same time. The AutoML model enables the researchers to just focus on the training time to deploy the model, which will improve the efficiency for shear strength prediction.

4.2. ML model error analysis

Based on previous description, R^2, RMSE and MAE are used to identify performance of seven models.

Fig. 4 shows values of metric error of seven ML models (red histogram is R^2, orange represent RMSE and green is MAE). Remarkably, the AutoML model surpasses all other models, demonstrating an R^2 value of 0.977, RMSE is 55.61 and an MAE value of 36.75 KN. Conversely, the foundational machine learning model, KNN, presents less favorable results with an R^2 of 0.877, RMSE of 128.57, and MAE of 69.85. Other models like XT, NN, RF, XGBoost and GBM also have commendable performance.

Table 2 illustrates the model error margins for different models. The statistical properties of the model error, including its mean and standard deviation, serve as crucial indicators of the bias and dispersion inherent in model predictions. In our investigation, the application of Automated Machine Learning (AutoML) demonstrates superior performance concerning model error, exhibiting mean,

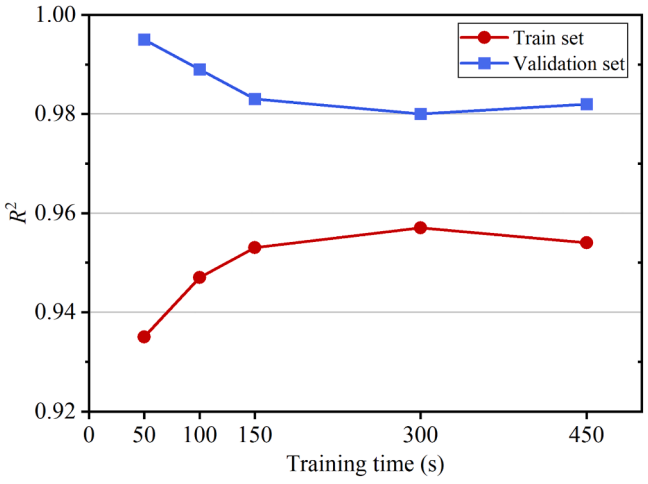

Fig. 3. Model performance versus the provided training time.

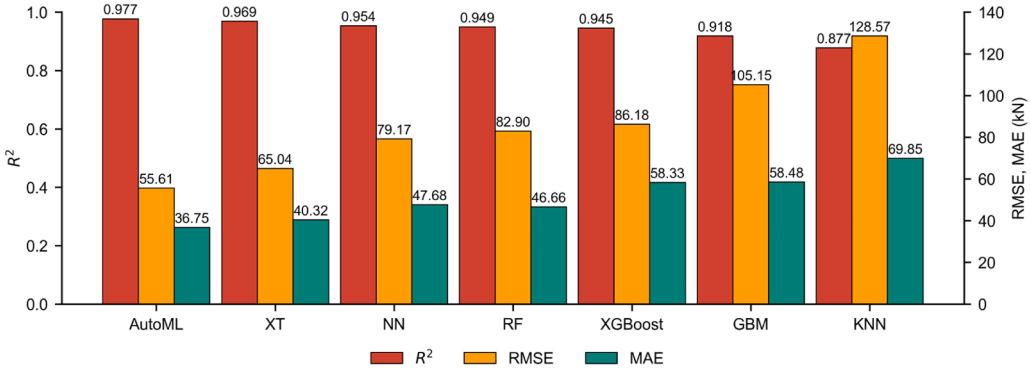

Fig. 4. Metrics error of ML model. Performance metrics comparison of machine learning models for shear strength prediction: (a) R^2, (b) RMSE, and (c) MAE. The models evaluated include AutoML, XT, NN, RF, XGBoost, GBM, and KNN. Higher R^2 values (closer to 1) and lower RMSE/MAE values indicate better predictive performance.

standard deviation and coefficient of variation of 0.999, 0.191 and 0.191, respectively. Conversely, the individual K-Nearest Neighbors (KNN) model displays the least favorable outcomes among the ensemble base models evaluated. Following AutoML, Gradient Boosting Machines (GBM) emerge as the next most effective model, yielding a mean, standard deviation and coefficient of variation of 0.982, 0.198 and 0.201, respectively. The findings underscore the efficacy of the AutoML model in mitigating both bias and variance inherent in base models via its integration strategy. This enhancement substantially bolsters the accuracy and reliability of AutoML, particularly evident in its predictive capabilities for shear strength.

Fig. 5 shows a violin diagram depicting the model error distribution of seven machine learning methods. The red dots at the center of each violin represent the average value, while the scattered dots of various colors represent the distribution of error values. The error values for all models cluster around 1, as depicted in Fig. 5, yet the mean error value for AutoML is the closest to 1. The red dot, symbolizing the mean, closely aligns with 1.0, coinciding with the red line (median), and revealing smaller upper and lower quartiles. This indicates a more centralized and homogeneous distribution of error values, resulting in a more concentrated violin shape. The XT model closely follows suit, with a red dot and red line near 1.0, but with a larger lower quartile and a relatively more erratic overall distribution. In contrast, other models, while marginally more accurate than KNN, exhibit skewed error distributions, extended tails, and broader upper and lower quartiles.

4.3. ML predictive performance analysis

This section discusses the results of the seven models on the test set in detail to verify the accuracy and generalization of the proposed model.

Fig. 6 presents a scatter plot comparing six predicted shear strength values (V_{pred}) with their corresponding experimental counterparts (V_{exp}), with the diagonal line representing perfect prediction parity. Points below this line denote conservative predictions. The broad distribution in the training set promotes model generalization, while the test set's broad distribution mitigates bias towards specific shear strength intervals. Most data points align closely with the ideal fit line, indicating strong agreement between predicted and experimental values, highlighting model's efficacy in shear strength prediction.

In Fig. 7, the histogram presents the distribution of model errors for the AutoML model, complemented by a corresponding kernel density estimate (KDE) curve. Notably, the average errors for both the training and test sets, registering at 0.999 and 0.977 respectively, closely approach unity, affirming the strong statistical alignment between AutoML-predicted values and experimental observations, indicative of exceptional model performance. Furthermore, scatter points from alternative models within the test set exhibit a tight clustering around the regression line, with the ranking based on the accuracy metric R^2as XT>NN>RF>XGBoost>GBM>KNN, highlighting the superior predictive prowess of AutoML while also showcasing competitive performance from other models.

Table 2
Model error of ML models.

	mean	std	cov
AutoML	0.999	0.191	0.191
XT	0.986	0.203	0.206
NN	1.057	0.258	0.244
RF	1.002	0.210	0.210
XGBoost	0.964	0.254	0.264
GBM	0.982	0.198	0.201
Knn	1.018	0.285	0.280

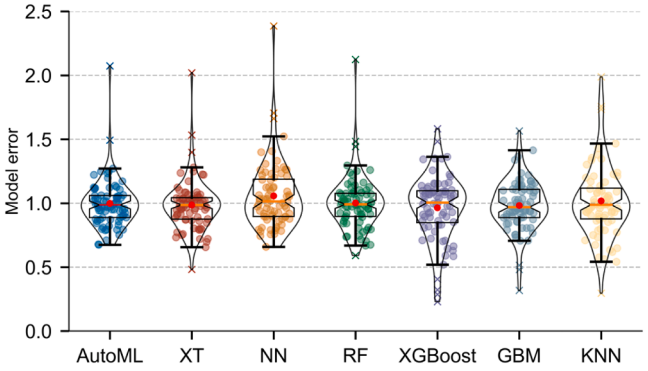

Fig. 5. Model error of ML models. The red dots at the center of each violin represent the average value, while the scattered dots of various colors represent the distribution of error values.

5. SHAP analysis

Incorporating AutoML and SHAP analysis in scientific papers offers significant benefits. SHAP analysis provides deep insights into each feature's contribution to a machine learning model's predictions, enhancing understanding of the model's decision-making process [53,54]. Meanwhile, AutoML simplifies tasks such as model selection, hyperparameter tuning, and feature engineering, reducing manual effort and time [55]. Together, AutoML and SHAP analysis enable researchers to efficiently explore complex models, identify key features, validate findings, and improve interpretability and transparency of research outcomes [56]. This integration facilitates informed decision-making, enhances reproducibility, and promotes the adoption of machine learning techniques across scientific domains.

5.1. Feature importance

As depicted in Fig. 8 below, SHAP analysis reveals that critical factors influencing shear strength are ranked as bo, h, d, fc, rho, fy, a, and b. Notably, the critical perimeter (bo), slab height (h), and effective depth (d) emerge as pivotal determinants of shear strength. The critical perimeter (bo) delineates the section in a structural element experiencing peak shear forces, pivotal for shear stress distribution. Slab height (h) directly impacts shear strength by providing a larger area to resist shear forces, with increased height correlating to greater strength. Effective depth (d), measured from compression fiber to tensile reinforcement centroid, enhances shear resistance efficiency. A larger effective depth augments the lever arm against shear forces, thus elevating shear strength. Importantly, the critical perimeter (bo) stands out as the most influential factor in SHAP analysis, with variations in bo significantly impacting shear stress distribution and consequent shear strength, surpassing the influence of alterations in slab height or effective depth.

Fig. 9 presents a comprehensive visualization encompassing a heatmap matrix displaying model output atop a grey dashed baseline, alongside a bar graph illustrating the global importance of each input factor in influencing shear strength. This depiction elucidates the hierarchical order of input significance, corroborating with the ascending importance exhibited in Fig. 8. Additionally, the heatmap encapsulates all 380 data points, unveiling the intricate relationship between selected factors and shear strength, aided by a color scale indicating relative impact. Notably, critical perimeter (bo) emerges as the foremost determinant of shear strength, with a discernible positive correlation observed within instances 0–130 and a subsequent negative trend. Fig. 10 further reinforces this, highlighting critical perimeter's pivotal role, while also delineating the contrasting impacts of other parameters, such as slab height (h) and effective depth (d), which positively influence shear strength, and shear span (a) and equivalent column width (b), which exhibit negative effects in alignment with conventional understanding.

SHAP can also provide a local explanation for each individual prediction, which can be particularly useful in understanding the impact of specific features on the prediction. Two instances of local explanation for shear strength prediction are illustrated in Fig. 11 using a waterfall plot. Each arrow in the figure denotes the direction and size of the influence of a feature on the prediction. The plot begins with the average of the output values E[f(x)] at the bottom. According to the principle of linear additivity, the outcome of each feature's contribution is added together to provide the final prediction.

A comparison of the two figures reveals some interesting contrasts. In the first scenario, the parameter bo has a positive impact of + 15.88 on the shear strength, while in the second scenario, it exerts a negative impact of −9.7. Conversely, rho demonstrates a significant negative influence of −33.43 in the Fig. 11 (a) but shows a substantial positive effect of + 40.93 in the Fig. 11 (b). Furthermore, the parameter fc exhibits a moderate positive contribution of + 9.15, which escalates to + 84.65 in the Fig. 11 (b).

These local explanations provide valuable insights into the specific factors that influence shear strength prediction. The observed contrasts indicate that the impact of each parameter can vary significantly depending on the context. For instance, the positive effect of fc is much more pronounced in the second scenario, suggesting a higher sensitivity to this parameter under different conditions. Similarly, the reversal of rho's impact from negative to positive underscores the importance of context-dependent interactions among parameters.

The local explanation of SHAP enables an intuitive understanding of the role of each feature in each prediction, thus making the

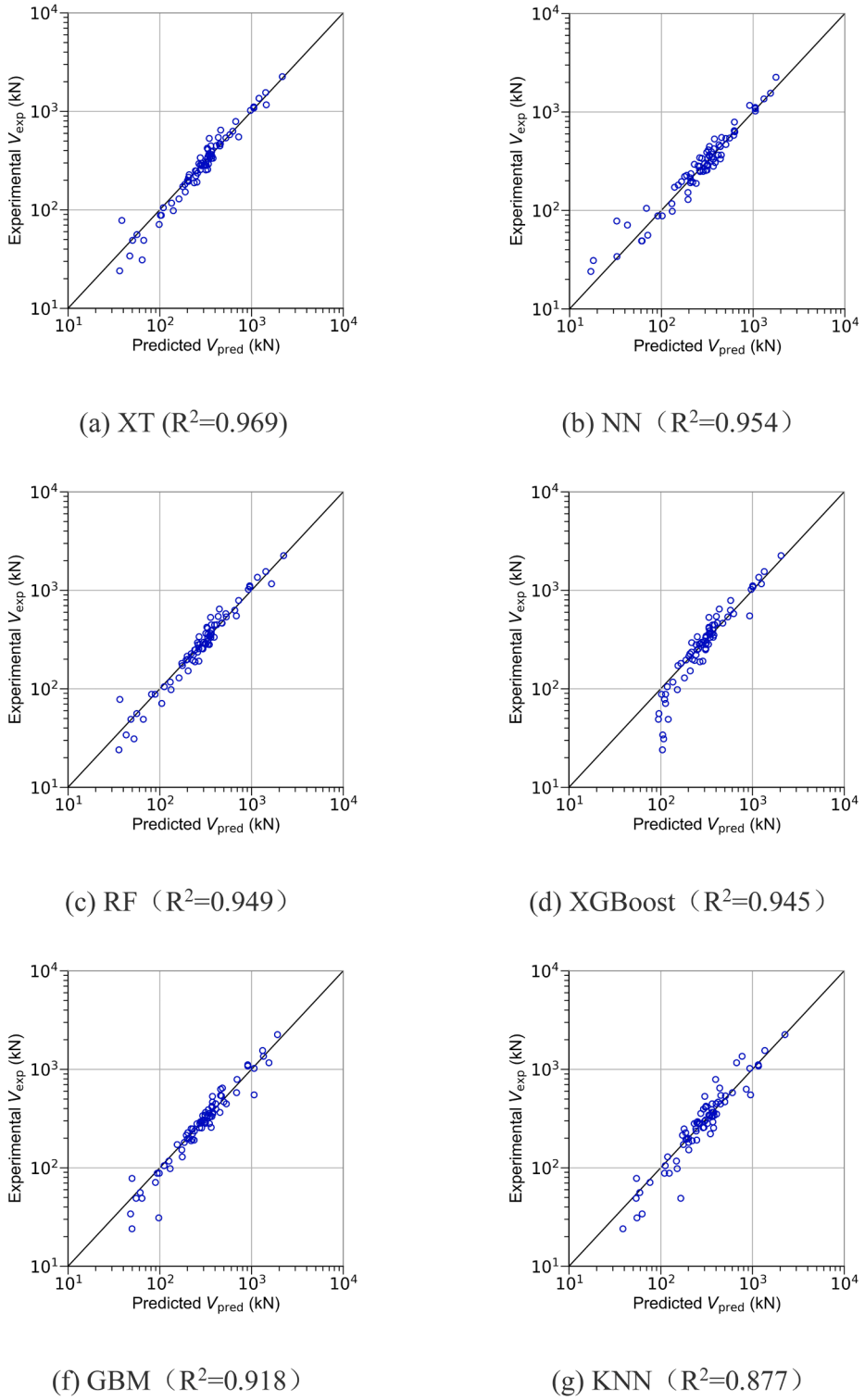

Fig. 6. Performance and comparison of machine learning models.

prediction process transparent. This allows us to see which features are most important in each prediction and how they contribute to the overall prediction. Additionally, the local explanation of SHAP can serve to explain the origin of a particular prediction and to identify any potential errors in the prediction process. The incorporation of feedback data into the prediction process through SHAP's local explanations can also improve the accuracy of the predictions.

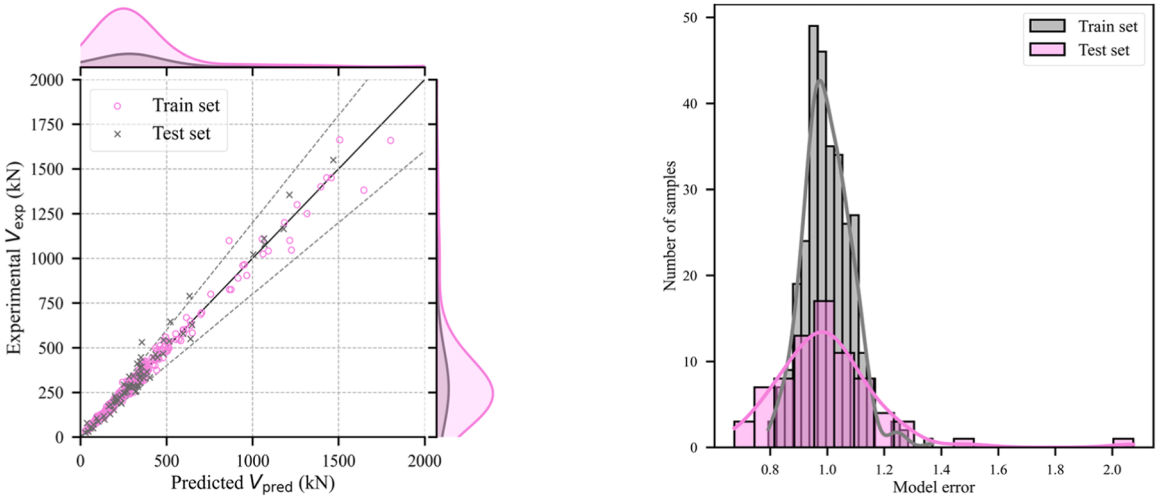

Fig. 7. Performance of AutoML (R^2=0.999, 0.977).

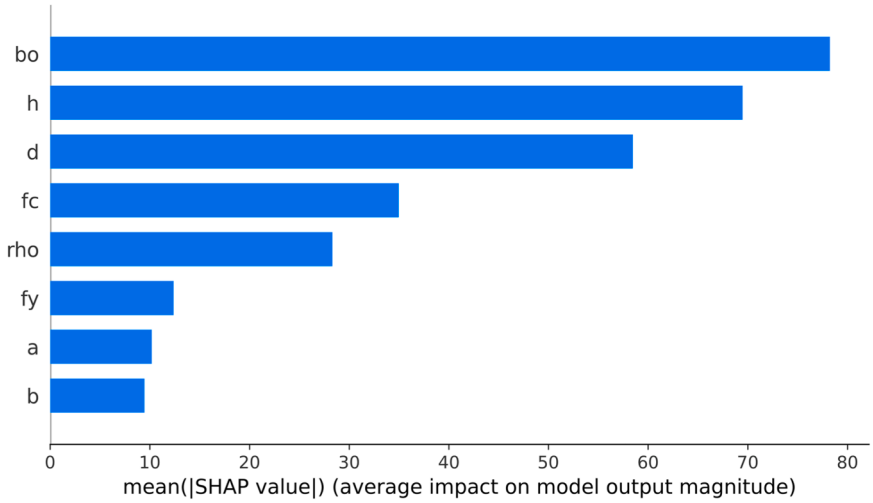

Fig. 8. Mean SHAP values using AutoML.

5.2. *Sensitivity analysis*

This section focuses on the analysis of SHAP dependency graphs. The significance of this analysis lies in its ability to provide comprehensive explanations for machine learning model predictions by visually illustrating the impact of features [57–59]. It enhances understanding of feature contributions, supports effective feature engineering, and aids in model refinement. By identifying key features and revealing their interactions, SHAP dependency graphs promote transparency, interpretability, and trust in model outcomes [60].

The SHAP dependency graph presented in Fig. 12 provides a comprehensive visualization of the influence and interdependencies of eight key factors, including the critical perimeter (bo), slab height (h), effective depth (d), compressive strength (fc), density (rho), yield strength of flexural reinforcement (fy), shear span (a), and equivalent column width (b), on the predictions generated by the machine learning model. Each factor is depicted as a node, and the connections between nodes indicate their relationships. By analyzing the associated SHAP values, the relative importance and contributions of each factor can be discerned, aiding in the interpretation of the model's decision-making process and providing insights into the intricate relationships and interactions among the factors.

The analysis reveals that the equivalent column width (bo), height (h), and effective depth (d) exhibit a positive influence on plate shear strength prediction, with increasing values of these features leading to higher shear strength predictions. This indicates that wider, taller, and deeper columns contribute to enhanced shear resistance. Conversely, the compressive strength (fc), density (rho), and yield strength of flexural reinforcement (fy) initially have a negative impact on plate shear strength prediction for small input

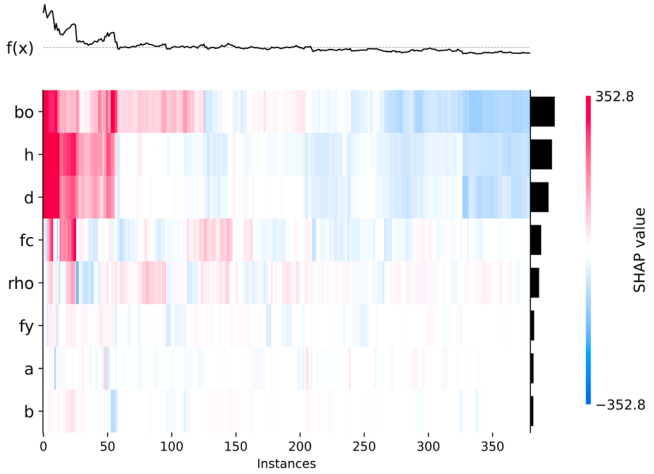

Fig. 9. Overall importance of input features.

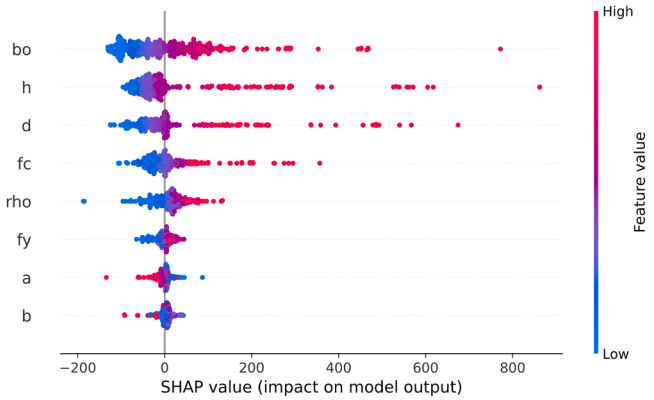

Fig. 10. Feature beeswarm plot.

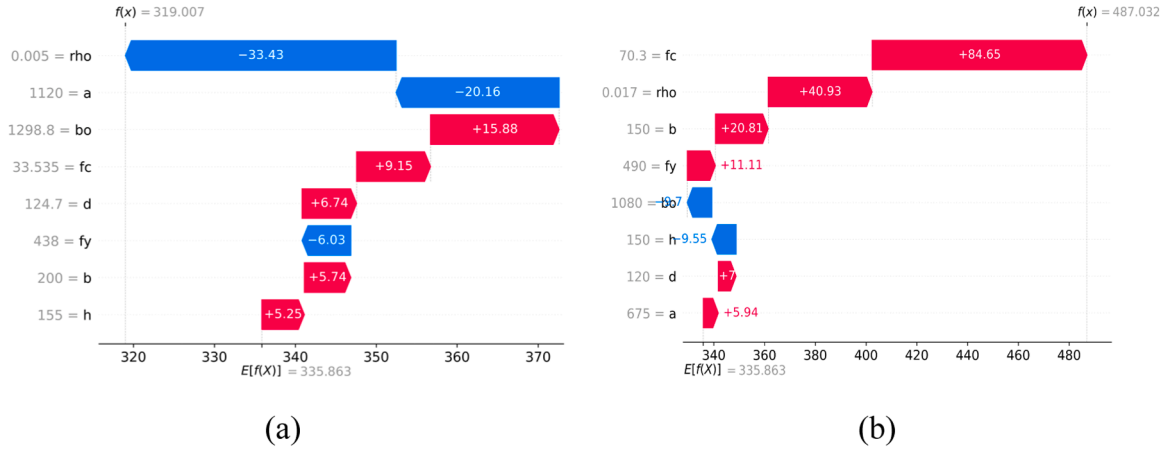

Fig. 11. Instances of local explanation based on SHAP.

values, but as these features increase, they start to positively influence the results, highlighting the significance of strong and dense materials in enhancing shear resistance. Notably, the equivalent column width (b) demonstrates a distinct spike in its prediction, maximizing its positive effect until a certain threshold, beyond which it negatively impacts the results. This suggests an optimal range for b that maximizes its contribution to shear strength, beyond which increasing b may reduce shear strength. Additionally, the shear

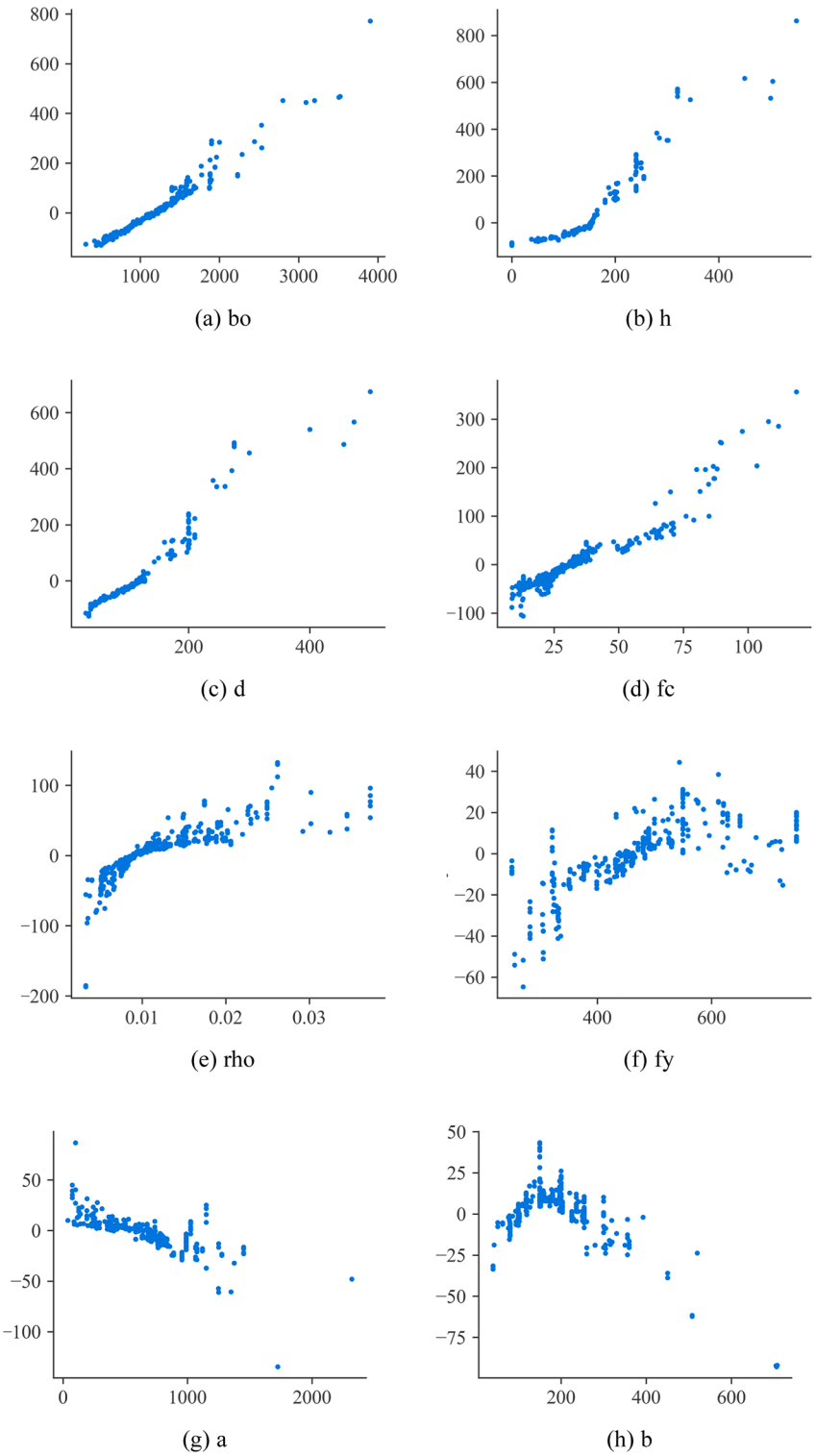

Fig. 12. SHAP Dependency Plot using ML Model.

span (a) exhibits a negative correlation with shear strength prediction, indicating that increasing the span length decreases shear strength.

The SHAP interaction values Fig. 13 is a novel attribution method that directly represents feature interactions, which are not captured by current methods. By extending SHAP values using the Shapley interaction index, we introduce SHAP interaction values.

These values ensure consistency and explain the interaction effects for individual predictions. They quantify the degree of interaction between features and can be used to measure interaction strength and visualize feature dependencies. The graph automatically identifies features with strong interactions and visualizes their relationships. This method enhances our understanding of feature interactions, aiding interpretation, model optimization, and decision explanation.

The SHAP interaction values, represented in Fig. 13, elucidate the relationships among four pairs of influences (bo vs h, h vs d, d with h, and fc vs h). Notably, bo vs h, h vs d, and d with h exhibit a positive correlation with the increasing shear strength of the plate, signifying that an escalation in the value of one feature corresponds to an increase in the value of the other feature. However, a distinctive variation is observed in the association between fc and h compared to the aforementioned correlations. Initially, as fc increases, it negatively impacts the shear strength of the plate, but this effect transitions to a positive one subsequently. Conversely, h displays a more discrete distribution, indicative of a positive correlation between the two features. Nevertheless, this relationship may not be straightforward, as it might be influenced by other factors exhibiting a non-linear relationship. Hence, a more comprehensive analysis is imperative to elucidate the characteristics and mechanisms of the relationship between fc and h, considering the potential influence of other factors and exploring the non-linear nature inherent in their relationship. Through such a meticulous analysis, a deeper comprehension of the intricate dynamics between these features and their implications for the shear strength of the plate can be garnered [61,62].

6. Preliminary development of prediction application

Building upon the insights and findings elucidated in Section 5 regarding RC slab shear strength prediction analysis, this section endeavors to refine and expand the automated methodology for enhanced evaluation of RC slab shear strength under varied conditions. Central to this objective is the application of a meticulously devised procedure tailored to the selected prediction methodology. By further optimizing the established framework, this section aims to provide a systematic and efficient means of characterizing the key factors influencing shear strength, thereby advancing our understanding and capabilities in structural performance assessment and design optimization.

6.1. Application description

In this study, PyQt5 [63], a Python framework based on the Qt library, was utilized to construct a robust software application tailored for the computation of plate shear strength across a diverse array of compositions. This software was meticulously crafted to enable user interaction, affording manipulation of ratios pertaining to fundamental components, including the equivalent column width [mm] (b), slab height [mm] (h), effective depth [mm] (d), critical perimeter [mm] (bo), shear span [mm] (a), density [kg/m^3] (rho), yield strength of flexural reinforcement [MPa] (fy), and compressive strength [MPa] (fc), as depicted in Fig. 14. The graphical user interface (GUI) developed through PyQt5 offers an intuitive platform featuring input fields and output parameters. Upon activation of the "Predict" function, the program harnesses PyQt5 to seamlessly execute backend calculations, furnishing users with a comprehensive analysis of plate shear strength across various compositional scenarios. This amalgamation of PyQt5 not only expedites software development but also engenders a user-friendly tool conducive to efficient plate shear strength computations. The program's user-centric interface, coupled with robust computational capabilities, furnishes a versatile solution for researchers and practitioners engaged in shear strength analysis, thereby offering valuable insights into the mechanical properties of diverse composition sets.

Fig. 15 presents a comparative analysis between experimentally measured shear strength values and those predicted by the computational prediction application. The strong correlation between the experimental and predicted data across all specimens highlights the model's high accuracy. This consistent agreement across multiple samples underscores the robustness and reliability of the prediction algorithm, affirming its effectiveness in accurately estimating shear strength. These results suggest the prediction program's potential utility for broader applications in related fields.

7. Conclusion

This study presents a robust and fully automated machine learning (AutoML) framework for predicting the punching shear strength of reinforced concrete (RC) slabs, with a particular focus on applications in marine structures. By adopting a multi-layer stacking ensemble that integrates multiple base learners, the proposed framework overcomes the limitations of traditional manual modeling approaches, including the inefficiencies associated with model selection and hyperparameter tuning. The AutoML system not only enhances predictive accuracy but also facilitates rapid, user-independent deployment, making it highly practical for real-time structural assessments in both conventional and aggressive marine environments.

Comparative evaluation against six individual machine learning models confirms that the AutoML framework consistently outperforms baseline approaches in terms of both prediction accuracy and computational efficiency. A dedicated prediction tool was also developed to translate the trained AutoML model into a user-friendly application, enabling fast and reliable shear strength estimation for practical engineering use cases. This feature is particularly relevant for marine infrastructure, where early identification of structural vulnerability is essential due to exposure to chloride-induced corrosion, wave-induced dynamic loading, and fluctuating environmental stressors.

(1) The AutoML model—based on a multi-level stacking strategy incorporating seven machine learning algorithms—demonstrates significantly higher accuracy than single-model techniques, validating the benefits of automated selection and optimization. Its

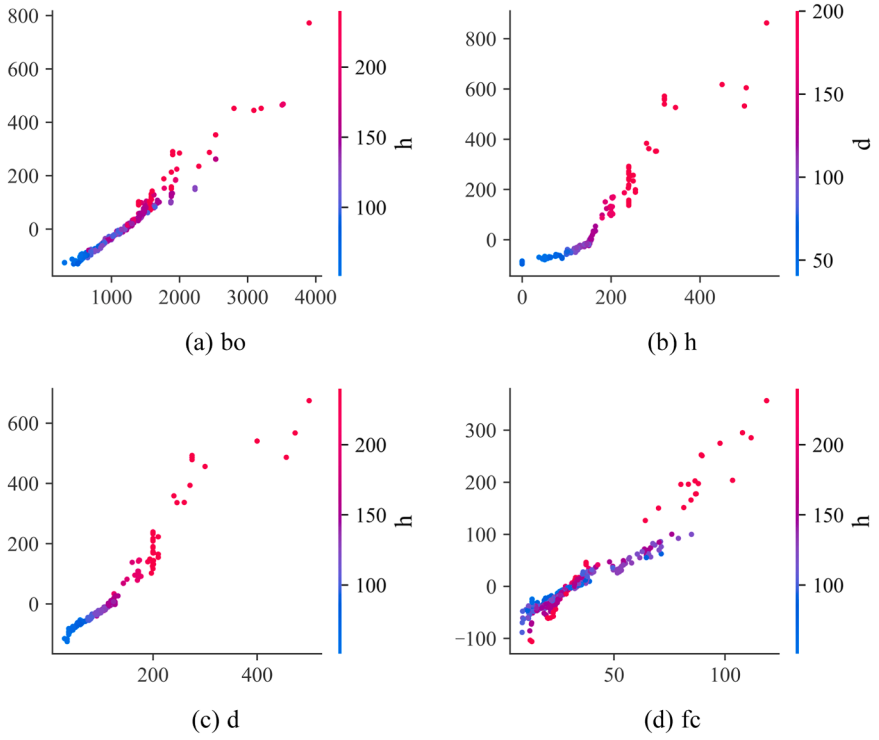

Fig. 13. SHAP Dependency Plot using ML Model.

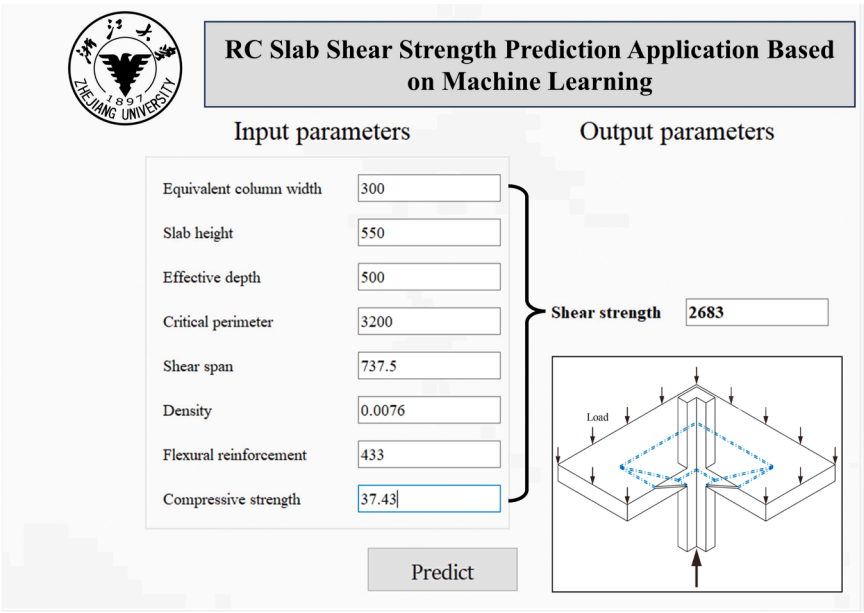

Fig. 14. Preliminary development of prediction application.

ability to harness diverse learning patterns makes it particularly suitable for complex structural scenarios, such as those encountered in offshore platforms, port facilities, and coastal defenses.

(2) Deployment is streamlined through a time-constrained training protocol, wherein a 150-second training window was found to balance computational cost and model precision effectively. This level of automation ensures minimal manual intervention while maintaining performance, making it viable for time-sensitive structural monitoring in remote or resource-limited marine contexts.

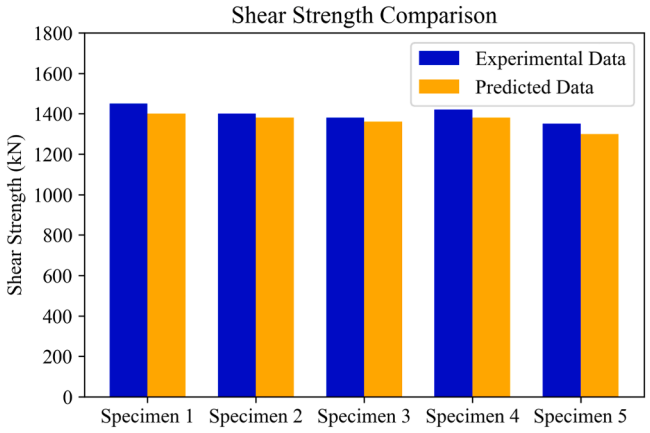

Fig. 15. Comparison of Experimental and Predicted data in prediction application.

(3) Error distribution analysis reveals that the AutoML framework achieves near-unity average error levels for both training and testing sets, further underscoring its robustness and generalizability across different data regimes, including those influenced by marine exposure.
(4) Model interpretability, achieved via SHAP (SHapley Additive exPlanations) analysis, highlights critical perimeter (bo), slab height (h), and effective depth (d) as the most influential parameters. The dominant role of the critical perimeter in shear strength prediction emphasizes its engineering relevance, especially for marine structures where dimensional optimization must account for long-term durability under corrosive conditions.
(5) The proposed framework establishes a scalable, data-driven methodology that not only improves prediction performance but also provides actionable insights for the design, assessment, and maintenance of RC slabs under variable environmental demands. Its adaptability to marine-specific deterioration mechanisms further enhances its practical utility in the context of resilient coastal and offshore infrastructure systems.

In summary, the integration of advanced ensemble learning with automated model optimization enables the proposed AutoML framework to deliver high-precision, interpretable, and deployment-ready predictions of RC slab shear strength. Its proven applicability to marine structures positions it as a valuable decision-support tool for structural engineers aiming to improve safety, reliability, and service life in challenging environmental conditions.

CRediT authorship contribution statement

Junwei Ren: Writing – original draft, Investigation, Data curation. **Ji XiaoHua:** Writing – review & editing. **Bin Jia:** Validation, Resources. **Gao Ziyue:** Software, Project administration. **Peng Xia:** Writing – review & editing. **Peng KaiDi:** Software. **Jingyu Wei:** Writing – original draft, Investigation, Data curation. **Bingcheng Chen:** Validation, Methodology, Formal analysis. **Sui Zijian:** Validation, Formal analysis.

Declaration of Competing Interest

The authors declare that they have no known competing financial interests or personal relationships that could have appeared to influence the work reported in this paper.

Acknowledgements

The authors acknowledge the financial support from the National Natural Science Foundation of China (Grant number: 12172244), a Project Supported by Scientific Research Fund of Zhejiang Provincial Education Department (Grant number: Y202352119), and the Talent Introduction Project of Zhejiang Shuren University (Grant number: 2024R038).

Data availability

Data will be made available on request.

References

[1] S. Eleftheriadis, P. Duffour, B. Stephenson, D. Mumovic, Automated specification of steel reinforcement to support the optimisation of RC floors, Autom. Constr. 96 (2018) 366–377.

[2] M. Q.u.Z. Khan, A. Ali, A. Ahmad, M. Raza, Iqbal, Experimental and finite element analysis of hybrid fiber reinforced concrete two-way slabs at ultimate limit state, Appl. Sci. 3 (1) (2021).
[3] M. Curbach, J. Hegger, J. Bielak, C. Schmidt, S. Bosbach, S. Scheerer, M. Claßen, J.W. Simon, H.G. Maas, A. Vollpracht, A. Koch, L. Hahn, M. Butler, B. Beckmann, V. Adam, C. Cherif, R. Chudoba, T. Gries, E. Günther, M. Kaliske, S. Klinkel, S. Löhnert, T. Lautenschläger, T. Matschei, V. Mechtcherine, W. E. Nagel, C. Neinhuis, A. Niemeyer, J.R. Noennig, M. Raupach, S. Reese, C. Scheffler, F. Schladitz, M. Traverso, S. Marx, New perspectives on carbon reinforced concrete structures—Why new composites need new design strategies, Civ. Eng. Des. 5 (5-6) (2024) 67–94.
[4] J. Liu, Z. Zou, K. Gao, J. Yang, S. He, Z. Wu, A novel digital unit cell library generation framework for topology optimization of multi-morphology lattice structures, Compos. Struct. 354 (2025) 118824.
[5] K. Chen, D. Wu, L. Xia, Q. Cai, Z. Zhang, Geopolymer concrete durability subjected to aggressive environments - a review of influence factors and comparison with ordinary portland cement, Constr. Build. Mater. 279 (2021) 122496.
[6] O.A. Mohamed, M. Kewalramani, R. Khattab, Fiber reinforced polymer laminates for strengthening of rc slabs against punching shear: a review, Polymers 12 (3) (2020).
[7] F. Cavagnis, M. Fernández Ruiz, A. Muttoni, Shear failures in reinforced concrete members without transverse reinforcement: an analysis of the critical shear crack development on the basis of test results, Eng. Struct. 103 (2015) 157–173.
[8] N.F. Zamri, R.N. Mohamed, D. Awalluddin, R. Abdullah, Experimental evaluation on punching shear resistance of steel fibre reinforced self-compacting concrete flat slabs, J. Build. Eng. 52 (2022).
[9] M.M.G. Inácio, M. Lapi, A.P. Ramos, Punching of reinforced concrete flat slabs - rational use of high strength concrete, Eng. Struct. 206 (2020).
[10] J. Einpaul, C.E. Ospina, M.F. Ruiz, A. Muttoni, Punching shear capacity of continuous slabs, Acids Struct. J. 113 (4) (2016) 861–872.
[11] S. Lips, M.F. Ruiz, A. Muttoni, Experimental investigation on punching strength and deformation capacity of shear-reinforced slabs, Acids Struct. J. 109 (6) (2012) 889–900.
[12] A. Marí, A. Cladera, E. Oller, J.M. Bairán, A punching shear mechanical model for reinforced concrete flat slabs with and without shear reinforcement, Eng. Struct. 166 (2018) 413–426.
[13] J. Wei, T. Shen, K. Wang, J. Liu, S. Wang, W. Hu, Transfer learning framework for the wind pressure prediction of high-rise building surfaces using wind tunnel experiments and machine learning, Build. Environ. 271 (2025) 112620.
[14] K. Wang, T. Shen, J. Wei, J. Liu, W. Hu, An intelligent framework for deriving formulas of aerodynamic forces between high-rise buildings under interference effects using symbolic regression algorithms, J. Build. Eng. 99 (2025) 111614.
[15] K.Y. Chen, J. Xia, R.J. Wu, X.Y. Shen, J.J. Chen, Y.X. Zhao, W.L. Jin, An overview on the influence of various parameters on the fabrication and engineering properties of CO2-cured cement-based composites, J. Clean. Prod. 366 (2022) 132968.
[16] R.Z. Alrousan, Ba.R. Alnemrawi, The influence of concrete compressive strength on the punching shear capacity of reinforced concrete flat slabs under different opening configurations and loading conditions, Struct 44 (2022) 101–119.
[17] D.W. Menna, A.S. Genikomsou, Punching shear response of concrete slabs strengthened with ultrahigh-performance fiber-reinforced concrete using finite-element methods, Pract. Period. Struct. Des. Constr. 26 (1) (2021).
[18] K. Wang, J. Liu, Y. Quan, Z. Ma, J. Chen, Y. Bai, Intelligent evaluation of interference effects between tall buildings based on wind tunnel experiments and explainable machine learning, J. Build. Eng. 96 (2024) 110449.
[19] K.Y. Chen, Y.Q. Wang, W.L. Min, J.J. Chen, R.J. Wu, Y. Peng, Y.X. Zhao, J. Xia, Performance characteristics of micro fiber-reinforced ambient cured one-part geopolymer mortar for repairing, Constr. Build. Mater. 415 (2024) 135086.
[20] A.A. Elshafey, E. Rizk, H. Marzouk, M.R. Haddara, Prediction of punching shear strength of two-way slabs, Eng. Struct. 33 (5) (2011) 1742–1753.
[21] A.M. Said, Y. Tian, A.A. Hussein, Evaluating punching shear strength of slabs without shear reinforcement using artificial neural networks, Am. Concr. Ins. Conv. 287 (2012) 1–18.
[22] A.H. Gandomi, D.A. Roke, Assessment of artificial neural network and genetic programming as predictive tools, Adv. Eng. Softw. 88 (2015) 63–72.
[23] V.-L. Tran, S.-E. Kim, A practical ANN model for predicting the PSS of two-way reinforced concrete slabs, Eng. Comput. 37 (3) (2020) 2303–2327.
[24] P. Chetchotisak, P. Ruengpim, D. Chetchotsak, S. Yindeesuk, Punching shear strengths of RC slab-column connections: prediction and reliability, KSCE J. Civ. Eng. 22 (8) (2017) 3066–3076.
[25] H.D. Nguyen, G.T. Truong, M. Shin, Development of extreme gradient boosting model for prediction of punching shear resistance of R/C interior slabs, Eng. Struct. 235 (2021).
[26] S. Mangalathu, H. Shin, E. Choi, J.-S. Jeon, Explainable machine learning models for punching shear strength estimation of flat slabs without transverse reinforcement, J. Build. Eng. 39 (2021).
[27] E. Alotaibi, O. Mostafa, N. Nassif, M. Omar, M.G. Arab, Prediction of punching shear capacity for fiber-reinforced concrete slabs using neuro-nomographs constructed by machine learning, J. Struct. Eng. 147 (6) (2021).
[28] S. Lu, M. Koopialipoor, P.G. Asteris, M. Bahri, D.J. Armaghani, A novel feature selection approach based on tree models for evaluating the punching shear capacity of steel Fiber-Reinforced concrete flat slabs, Mater 13 (17) (2020).
[29] N.-D. Hoang, Estimating punching shear capacity of steel fibre reinforced concrete slabs using sequential piecewise multiple linear regression and artificial neural network, Measurement 137 (2019) 58–70.
[30] D.-T. Vu, N.-D. Hoang, Punching shear capacity estimation of FRP-reinforced concrete slabs using a hybrid machine learning approach, Struct. Infrastruct. Eng. 12 (9) (2015) 1153–1161.
[31] I. Faridmehr, M.L. Nehdi, M. Hajmohammadian Baghban, Novel informational bat-ANN model for predicting punching shear of RC flat slabs without shear reinforcement, Eng. Struct. 256 (2022).
[32] D. Zhang, Y. Shen, Z. Huang, X. Xie, Auto machine learning-based modelling and prediction of excavation-induced tunnel displacement, J. Rock. Mech. Geotech. Eng. 14 (4) (2022) 1100–1114.
[33] Q. Zhang, W. Hu, Z. Liu, J. Tan, TBM performance prediction with Bayesian optimization and automated machine learning, Tunn. Undergr. Space Technol. 103 (2020).
[34] Z. Zou, J. Liu, K. Gao, D. Chen, J. Yang, Z. Wu, Inverse design of functionally graded porous structures with target dynamic responses, Int. J. Mech. Sci. 280 (2024) 109530.
[35] S. Wang, J. Liu, Q. Wang, R. Dai, K. Chen, Prediction of non-uniform shrinkage of steel-concrete composite slabs based on explainable ensemble machine learning model, J. Build. Eng. 88 (2024) 109002.
[36] K.Y. Chen, R.Y. Lan, T.Q. He, P.R. Heng, J. Xia, Evaluation on reactivity of Fly ash from different sources in alkali activated system-progressing environmentally construction through waste utilization, Constr. Build. Mater. 454 (2024) 139118.
[37] A. Truong, A. Walters, J. Goodsitt, K. Hines, C.B. Bruss, R. Farivar, Towards automated machine learning: evaluation and comparison of automl approaches and tools, 2019 IEEE 31st Int. Conf. Tools Artif. Intell. (ICTAI) (2019) 1471–1479.
[38] J. Waring, C. Lindvall, R. Umeton, Automated machine learning: review of the state-of-the-art and opportunities for healthcare, Artif. Intell. Med. 104 (2020) 101822.
[39] K.Y. Chen, C. Miao, G.H. Lyu, K.X. Wu, J.J. Chen, J. Xia, Developing an indexing methodology for estimating the reactivity of slag from different sources use in alkali-activated materials, J. NonCryst. Solids 647 (2025) 123278.
[40] H. Adeli, Neural networks in civil engineering: 1989-2000, Comput.-Aided Civ. Infrastruct. Eng. 16 (2) (2001) 126–142.
[41] M. Amiri, H. Bakhshandeh Amnieh, M. Hasanipanah, L.Mohammad Khanli, A new combination of artificial neural network and K-nearest neighbors models to predict blast-induced ground vibration and air-overpressure, Eng. Comput. 32 (4) (2016) 631–644.
[42] B. Yu, X. Song, F. Guan, Z. Yang, B. Yao, K-nearest neighbor model for multiple-time-step prediction of short-term traffic condition, J. Transp. Eng. 142 (6) (2016).

[43] K. Chen, J. Xia, R. Wu, X. Shen, J. Chen, Y. Zhao, W. Jin, An overview on the influence of various parameters on the fabrication and engineering properties of CO2-cured cement-based composites, J. Clean. Prod. 366 (2022) 132968.
[44] M.M. Hameed, M.K. AlOmar, F. Khaleel, N. Al-Ansari, D. Armaghani, An extra tree regression model for discharge coefficient prediction: novel, practical applications in the hydraulic sector and future research directions, Math. Probl. Eng. 2021 (2021) 1–19.
[45] G. Biau, E. Scornet, A random forest guided tour, Test 25 (2) (2016) 197–227.
[46] R.P. Sheridan, W.M. Wang, A. Liaw, J. Ma, E.M. Gifford, Extreme gradient boosting as a method for quantitative structure-activity relationships, J. Chem. Inf. Model 56 (12) (2016) 2353–2360.
[47] S. Bergen, M.M. Huso, A.E. Duerr, M.A. Braham, S. Schmuecker, T.A. Miller, T.E. Katzner, A review of supervised learning methods for classifying animal behavioural states from environmental features, Methods Ecol. Evol. 14 (1) (2023) 189–202.
[48] A. Ahmad, F. Farooq, P. Niewiadomski, K. Ostrowski, A. Akbar, F. Aslam, R. Alyousef, Prediction of compressive strength of fly ash based concrete using individual and ensemble algorithm, Mater 14 (4) (2021).
[49] H.I. Erdal, O. Karakurt, E. Namli, High performance concrete compressive strength forecasting using ensemble models based on discrete wavelet transform, Eng. Appl. Artif. Intell. 26 (4) (2013) 1246–1254.
[50] A. Ahmad, W. Ahmad, F. Aslam, P. Joyklad, Compressive strength prediction of Fly ash-based geopolymer concrete via advanced machine learning techniques, Case Stud. Constr. Mater. 16 (2022).
[51] D. Chicco, M.J. Warrens, G. Jurman, The coefficient of determination R-squared is more informative than SMAPE, MAE, MAPE, MSE and RMSE in regression analysis evaluation, PeerJ Comput. Sci. 7 (2021) e623.
[52] D.L. Alexander, A. Tropsha, D.A. Winkler, Beware of R(2): simple, unambiguous assessment of the prediction accuracy of QSAR and QSPR models, J. Chem. Inf. Model 55 (7) (2015) 1316–1322.
[53] H. Kaur, H. Nori, S. Jenkins, R. Caruana, H. Wallach, J. Wortman Vaughan, Interpreting interpretability: understanding data scientists' use of interpretability tools for machine learning. Proceedings of the 2020 CHI Conference on Human Factors in Computing Systems, 2020, pp. 1–14.
[54] A. Singh, S. Sengupta, V. Lakshminarayanan, Explainable deep learning models in medical image analysis, J. Imaging 6 (6) (2020).
[55] V. Belle, I. Papantonis, Principles and practice of explainable machine learning, Front. Big Data 4 (2021) 688969.
[56] B. Sun, W. Cui, G. Liu, B. Zhou, W. Zhao, A hybrid strategy of AutoML and SHAP for automated and explainable concrete strength prediction, Case Stud. Constr. Mater. 19 (2023).
[57] V.V. Degtyarev, Machine learning models for predicting bond strength of deformed bars in concrete, Acids Struct. J. 119 (5) (2022) 43–56.
[58] A. Kashem, R. Karim, S.C. Malo, P. Das, S.D. Datta, M. Alharthai, Hybrid data-driven approaches to predicting the compressive strength of ultra-high-performance concrete using SHAP and PDP analyses, Case Stud. Constr. Mater. 20 (2024).
[59] P. Thisovithan, H. Aththanayake, D.P.P. Meddage, I.U. Ekanayake, U. Rathnayake, A novel explainable AI-based approach to estimate the natural period of vibration of masonry infill reinforced concrete frame structures using different machine learning techniques, Results Eng. 19 (2023).
[60] C. Zhang, Z. Zhu, F. Liu, Y. Yang, Y. Wan, W. Huo, L. Yang, Efficient machine learning method for evaluating compressive strength of cement stabilized soft soil, Constr. Build. Mater. 392 (2023).
[61] D.C. Feng, W.J. Wang, S. Mangalathu, E. Taciroglu, Interpretable XGBoost-shap machine-learning model for shear strength prediction of squat RC walls, J. Struct. Eng. 147 (11) (2021).
[62] I.U. Ekanayake, D.P.P. Meddage, U. Rathnayake, A novel approach to explain the black-box nature of machine learning in compressive strength predictions of concrete using shapley additive explanations (SHAP), Case Stud. Constr. Mater. 16 (2022).
[63] L.L. Gou, S.Q. Li, H. Miao, M. Gao, F.L. He, L.Y. You, Dots and boxes interactive interface implementation and algorithm improvement. 31st Chinese Control And Decision Conference (CCDC), Ieee, Nanchang, PEOPLES R CHINA, 2019, pp. 6270–6275.